Energy Calibration for the INDRA Multidetector Using Recoil Protons from ^{12}C + ^{1}H Scattering

A. Trzciński [a], J. Łukasik [b,c], W.F.J. Müller [b], W. Trautmann [b], B. Zwiegliński [a,*], G. Auger [d], Ch.O. Bacri [e], M.L. Begemann-Blaich [b], N. Bellaize [f], R. Bittiger [b], F. Bocage [f], B. Borderie [e], R. Bougault [f], B. Bouriquet [d], Ph. Buchet [g], J.L. Charvet [g], A. Chbihi [d], R. Dayras [g], D. Doré [g], D. Durand [f], J.D. Frankland [d], E. Galichet [h], D. Gourio [b], D. Guinet [h], S. Hudan [d], B. Hurst [f], P. Lautesse [h], F. Lavaud [e], J.L. Laville [d], C. Leduc [h], A. Le Fèvre [b], R. Legrain [g,1], O. Lopez [f], U. Lynen [b], L. Nalpas [g], H. Orth [b], E. Plagnol [e], E. Rosato [i], A. Saija [j], C. Schwarz [b], C. Sfienti [b], J.C. Steckmeyer [f], G. Tăbăcaru [d], B. Tamain [f], K. Turzó [b], E. Vient [f], M. Vigilante [i], C. Volant [g]

INDRA and ALADIN collaborations

[a] *The Andrzej Soltan Institute for Nuclear Studies, PL-00681 Warsaw, Hoża 69, Poland*

[b] *Gesellschaft für Schwerionenforschung mbH, D-64291 Darmstadt, Germany*

[c] *Henryk Niewodniczański Institute of Nuclear Physics, PL-31342 Cracow, Poland*

[d] *GANIL, CEA et IN2P3-CNRS, F-14076 Caen, France*

Preprint submitted to Elsevier Science *15 November 2002*

[e] *Institut de Physique Nucléaire, IN2P3-CNRS et Université, F-91406 Orsay, France*

[f] *LPC, IN2P3-CNRS, ISMRA et Université, F-14050 Caen, France*

[g] *DAPNIA/SPhN, CEA/Saclay, F-91191 Gif-sur-Yvette, France*

[h] *Institut de Physique Nucléaire, IN2P3-CNRS et Université, F-69622 Villeurbanne, France*

[i] *Dipartimento di Scienze Fisiche e Sezione INFN, Univ. Federico II, I-80126 Napoli, Italy*

[j] *Dipartimento di Fisica dell' Università and INFN, I-95129 Catania, Italy*

Abstract

An efficient method of energy scale calibration for the CsI(Tl) modules of the INDRA multidetector (rings 6 - 12) using elastic and inelastic ^{12}C + ^{1}H scattering at $E(^{12}\mathrm{C}) = 30$ MeV per nucleon is presented. Background-free spectra for the binary channels are generated by requiring the coincident detection of the light and heavy ejectiles. The gain parameter of the calibration curve is obtained by fitting the proton total charge spectra to the spectra predicted with Monte-Carlo simulations using tabulated cross section data. The method has been applied in multifragmentation experiments with INDRA at GSI.

Key words: Charged particle spectroscopy, CsI(Tl) scintillation detectors, ^{12}C + ^{1}H scattering at 30 MeV per nucleon, Light-energy response for protons

PACS: 29.40.Mc, 29.30.Ep

* Corresponding author. Tel.: +(48) 22 5532138, fax: +(48) 22 6213829.
Email address: bzw@fuw.edu.pl (B. Zwieglíński).

[1] Deceased.

1 Introduction

The 4π multidetector INDRA [1] was commissioned in 1992 to perform multifragmentation studies with heavy-ion beams in the Fermi energy domain at the GANIL Laboratory. It has a granularity of 336 cells in solid-angle and a shell structure with several detection layers. The outermost layer consists of CsI(Tl) scintillators coupled to photomultiplier tubes (PMTs). Particle identification is achieved with the $\Delta E - E$ technique and by pulse shape analysis of the CsI(Tl) signals.

The calibration for the CsI(Tl) detectors consists in determining a function that relates the total charge collected in the PMT anode circuit, Q_0, to the energy, E_0, deposited by a particle in the scintillator. This information is needed for all particle species and over their energy ranges relevant for the experiment. The light response of CsI(Tl) to a charged particle of atomic number Z and mass number A is non-linear with respect to E_0, depending on Z and A. The non-linearity is caused by light-quenching and suggested to be proportional to the particle electronic stopping power in the scintillator according to the well-known Birks formula [2]. Parlog *et al.* proved Birks' conjecture in the framework of a recombination model and extended it to incorporate the effect of δ-rays, escaping from the excited and ionized column of atoms along the particle track [3]. They derived also an analytic approximation to their extended approach [4], expressing Q_0 as a function of E_0, Z and A with four parameters a_1, a_2, a_3 and a_4 [eq. (9) in the latter reference, referred to below as Parlog formula].

CsI(Tl) crystals with PMT or photodiode readout have been incorporated as

full energy detectors into many of the existing large solid angle multidetector arrays. For some of them the calibration procedures are also reported (see e.g. [5–10]). To describe the light response different analytical approximations to the Birks formula were applied, which include two [5,6], three [7,8], or four [9,10] parameters, depending on the range of particle species and their energies utilized in the calibration experiment.

The calibration procedure developed for INDRA at GANIL employed fragmentation products of the ^{16}O beam at 95 MeV per nucleon on a thick ^{12}C target located in the focus of the beam analysing system ALPHA [1,11]. The fragmentation products (Z = 1-6), selected in a relatively narrow (and variable) range of magnetic rigidity, were delivered into the center of the INDRA detector. Spectra of elastic scattering on Au, Ta or C targets were measured and then used as calibration data.

In 1997 INDRA has been transported to GSI (Darmstadt) in order to extend multifragmentation studies into the domain of higher projectile energies available from the heavy-ion synchrotron SIS-18. The calibration for this campaign was primarily obtained from a detector-by-detector intercomparison of α-particle spectra measured for the reaction ^{129}Xe + $^{\rm nat}$Sn at 50 MeV per nucleon at GSI with the energy spectra obtained for the same system and projectile energy at GANIL [12]. This provided calibration parameters a_1 and a_2 for all modules. The higher parameters a_3 and a_4 in the latter calibration procedure were obtained by fitting measured $\Delta E - E$ correlations with predictions of energy loss and range tables [13].

The series of experiments at GSI proceeded in three subcampaigns with beams of gold, xenon and carbon ions. Within each subcampaign, the stability of

the PMT gains was controlled with the laser system installed in the INDRA detector [1]. Possible gain changes between the subcampaigns were controlled with several methods. The highest intrinsic accuracy of better than 5% was achieved by requiring an optimum matching of the topological structure of the two-dimensional maps of fast and slow CsI(Tl) signals.

The ^{12}C + ^{1}H experiment at $E(^{12}\mathrm{C}) = 30$ MeV per nucleon, described in the present work, has been undertaken to provide proton energies to be used as an independent set of reference points in order to confirm the ^{129}Xe + $^{\mathrm{nat}}$Sn calibrations and to obtain a measure of their accuracies.

2 Calibration principle

2.1 Kinematics and geometry

The 4π multidetector INDRA [1] is segmented into 17 rings with azimuthal symmetry around the beam axis. Each ring is divided in azimuth, ϕ, into 8, 12, 16, or 24 detection cells which cover altogether 90% of the full solid angle. The axial symmetry and high coverage make it particularly well suited to perform energy calibrations using binary reactions because a coincidence requirement between the light (l) and the heavy (h) ejectile can be used to select specific channels. The selection of elastic and inelastic protons is detailed below.

Fig. 1 presents energies of the elastic and inelastic protons to the 4.439 MeV state of ^{12}C as functions of the emission polar angle for the incident energy $E(^{12}\mathrm{C}) = 30$ MeV per nucleon. The angles delimiting the acceptance in θ_{l} of the modules of consecutive INDRA rings are indicated with the vertical

dotted lines (the numbering follows the convention adopted in Ref. [1]). The choice of beam energy was primarily guided by the intention of having the corresponding proton ranges well within the length of CsI(Tl) crystals (see Table 2 in Ref. [1]), which decreases with increasing ring number. The width of an interval of proton energies within a detector, $E_{\rm l}$ in Fig. 1, increases with increasing ring number, reflecting the increasing width of the subtended polar angles and the slope variation of the $E_{\rm l}$ vs. $\theta_{\rm l}$ dependence. Dealing with a finite-geometry problem, we have decided to simulate the coincident light and heavy ejectile detection using a Monte-Carlo method. The simulated spectra serve as reference in the calibration procedure (see Sect. 3).

Fig. 2 shows the correlation between the emission polar angles $\theta_{\rm l}$ and $\theta_{\rm h}$. It defines the coincidence requirement for the selection of a specific reaction channel in a given module. The minimum detection angle $\theta_{\rm h} = 2^\circ$ for ^{12}C ejectiles reached within ring 1 (2°-3°) has the consequence that, for elastically scattered protons, the coincidence requirement can be met for rings 5 to 12 and, in practice, only for rings 6 to 12. The gain settings for the Si detectors in ring 5 were set too low in the current experiment to resolve hydrogen isotopes. The finite size of the beam spot and the energy loss of the projectile in the target cause a broadening of the sharp coincidence conditions displayed in the figure.

2.2 Monte-Carlo simulations

The purpose of the Monte-Carlo simulations is taking into account in a realistic way in the reference spectra energy losses and the finite solid angles encountered by the detected coincident particles. Inspection of Fig. 1 demonstrates

that the importance of these two factors increases with increasing detection angle.

We assume a parallel beam of ^{12}C projectiles illuminating uniformly a circular area of 10 mm diameter on a target foil of finite thickness. The coordinates of the reaction point are chosen randomly within the target volume. The interaction point marks the origin of a polar coordinate system having its z-axis oriented parallel to the beam axis. A light ejectile is emitted in the direction $\theta_{\rm l}, \phi_{\rm l}$ in this polar system, with the angle $\phi_{\rm l}$ drawn randomly, whereas $\theta_{\rm l}$ according to weights given by the cross section angular distribution. The angles $\theta_{\rm h}$ and $\phi_{\rm h}$ then result uniquely from the reaction kinematics. The particle trajectories are then transformed into the coordinate system centered at the beam axis and followed to the detectors.

The absolute differential cross sections $d\sigma/d\Omega$ for the elastic ^{12}C(p,p)^{12}C(g.s.) and inelastic ^{12}C(p,p')^{12}C(4.439 MeV) scattering were adopted from different sources with the stated energy close to $E_{\rm p} = 30$ MeV. The elastic data are from the ENDF/B-VI evaluated data file at $E_{\rm p} = 30.0$ MeV, accessible via the BNL National Nuclear Data Center. Two sets of the inelastic cross sections have been tested. The first set was taken from Ref. [14], where measurements were performed at $E_{\rm p} = 28.7$ MeV, while the second one from Ref. [15] reporting the results at $E_{\rm p} = 31.1$ MeV. The latter set was adopted in the simulations for the reason of its giving a much better fit to the data. Angular distributions $d\sigma/d\Omega$ are converted into energy distributions $d\sigma/dE$ within the program via $d\sigma/dE = d\sigma/d\Omega \cdot d\Omega/dE$, where $dE/d\Omega$ is given by the kinematics. One should stress that the quality of the fits depends in an essential way on the precision of the assumed cross sections (see Sect. 3).

Rings 2 to 9 of INDRA are composed of three successive detection layers, ionization chambers, silicon detectors and CsI(Tl) scintillators [1]. During the INDRA experiments at GSI, the original ring 1 consisting of plastic-scintillator phoswich detectors was replaced with a new ring composed of Si-CsI(Tl) $\Delta E - E$ modules. Energy losses suffered by the particles in the target and in the detector materials in front of the CsI(Tl) scintillators were determined by interpolating in tables of stopping powers and ranges calculated with the program SRIM-2000 of Ziegler [16].

3 Results of the calibration experiment

The measurements were performed with ^{12}C beams of 30 MeV per nucleon extracted from the SIS-18 synchrotron. These calibration runs were done within the subcampaign devoted to experiments with ^{197}Au beams. They followed directly after a series of production runs with ^{197}Au at 100 MeV per nucleon, and all high-voltage and gain settings were unmodified.

A polyethylene foil of areal density 20 mg/cm^2 was used as a target and the average beam intensity was $\approx 5 \cdot 10^8$ ions/sec. The diameter of the beam spot on target did not exceed 1 cm in the course of these measurements. The latter number was, therefore, assumed as the diameter of the illuminated beam spot in the simulations.

The data reduction procedure consisted of three steps. In the first step all double coincidences between Si and CsI(Tl) detectors have been extracted from raw data for all modules in rings 1 to 12. With each of these events three parameters are associated: Si-high gain, ΔE_{Si}, CsI(Tl)-fast signal, E_{F},

and CsI(Tl)-slow signal, $E_{\rm S}$. Fast-signal and slow-signal refer to amplitudes corresponding, respectively, to charges integrated within 0 - 390 ns and 1590 - 3090 ns from the start of the PMT current flow (see [17] for details of the INDRA electronics). Two-dimensional maps $\Delta E_{\rm Si} - E_{\rm F}$ and $\Delta E_{\rm Si} - E_{\rm S}$, for rings 6 to 12, gave orientation as to locations of the high-$E_{\rm F,S}$ ends of the proton hyperbolae, where the calibration peaks were expected to occur and defined the ranges of energy scales (in channels) to be taken into account in the subsequent steps of the analysis. The second step extracted from this reduced set, for each given module Si-CsI-light (l) in rings 6 to 12, fourfold coincidences with the Si-CsI-heavy (h), the one which fulfilled the angular constraints dictated by kinematics for the elastic and inelastic scattering of ^{12}C projectiles on target protons. For the latter set of events the $E_{\rm F}$ and $E_{\rm S}$ parameters were converted into total-charge, Q_0, collected throughout the entire scintillation, using the weights resulting from eqs. 4 and 5 in [4]. In the coincident spectra at more forward angles the proton groups of interest are already well separated, as is evident from the comparison of Fig. 3b with Fig. 3a. A background-free selection was achieved in the third step by requesting a coincidence with a carbon ion, and the resulting proton yields were then extracted by imposing two-dimensional gates and projecting the gated area onto the Q_0-axis, as required by the Parlog formula (see Sect. 1). No discrete lines were identified in the projected deuteron spectrum, therefore deuteron-based calibrations are not addressed further in the present work.

Figs. 4a-h present a sample of calibrated proton spectra, fitted to the corresponding Monte-Carlo results, for individual detector modules from rings 6 to 12 in coincidence with the complementary modules from rings 1 to 3. One may follow the shape variations of the spectra with increasing ring number. In the

forwardmost ring 6 accessible with the present method (Fig. 4a), the proton spectrum is of "narrow-geometry" type, resulting in well-defined calibration peaks. The higher yield of the inelastic peak relative to the elastic one is a characteristic feature of the p + ^{12}C scattering into the backward hemisphere around $E_{\rm p} = 30.0$ MeV [14,15]. Fig. 4h is representative for "wide-geometry" spectra, in which the effects of finite solid angle and energy losses of protons in the traversed materials are maximum, causing a significant smearing of the elastic peak. The ^{12}C(4.439 MeV) inelastic peak no longer contributes at these large proton detection angles (see Figs. 1 and 2). At intermediate angles (Figs. 4b-g) both peaks may be present, depending on the coincidence requirement (Figs. 4e-f). Here the inelastic peak is of lower intensity than the elastic peak (Fig. 4e). The evolution of the spectra shapes is very well reproduced, as seen in Figs. 4a-h, with the Monte-Carlo simulations.

4 Comparison of gain factors and centroid energies

The fast protons, detected in rings 6 - 12, are to a large extent insensitive to nonlinear effects in the light production, and no attempt was made to deduce higher calibration coefficients from the spectra. The coefficients $a_2 - a_4$ were fixed at the values adopted for protons in the analysis of the main experiment [12], and only the coefficient a_1 was varied in the fitting procedure. In Fig. 4 the obtained excellent agreement is demonstrated for the examples given there. The resulting a_1 coefficients for these cases and their intrinsic errors, due to the fitting procedure itself, are collected in the second column of Table 1. Note, however, that the spectra used to extract the listed a_1 coefficients had Q_0 scales expanded in comparison with those presented in Fig. 3. The

errors of a_1's are generally near or below 2% even for the most unfavorable case of ring 12. The third column lists the corresponding set of a_1 parameters obtained from the ^{129}Xe + ^{nat}Sn calibrations. The agreement is generally very good, not exceeding 3%, with the exception of the case 07-11 for which the deviation is near 5%.

This procedure was applied to nearly 170 modules of rings 6 to 12 which represent one half of all CsI(Tl) detectors of INDRA. The distribution of the differences in the centroid energies of proton spectra obtained with the two methods is given in Fig. 5. It is centered near a mean value close to zero and has a standard deviation of about 4%. This result may be considered a quantitative measure of the overall accuracy of the linear term of the energy scale calibration of the CsI(Tl) modules in this campaign. In particular, also the methods of following gain changes within a subcampaign and of controlling gain changes between the three subcampaigns [12] are included in this test.

5 Conclusions

Measurements of elastic and inelastic scattering of ^{12}C + ^{1}H at 30 MeV per nucleon have been performed in order to test the energy scale calibration of the CsI(Tl) detectors of the INDRA multidetector for the series of recent experiments performed at GSI. The binary channels were selected by requiring a coincidence between the light and heavy ejectiles, thereby exploiting the high solid-angle coverage of the INDRA multidetector. The so obtained background-free proton spectra were fitted to theoretical spectra obtained with a Monte-Carlo procedure using cross section data from the literature. The resulting linear calibration coefficients were found to have an intrinsic accuracy

better than 2%.

Because of the inverse kinematics of the scattering experiment the application of the method was limited to rings 6 to 12 of the INDRA detector ($\theta_{\rm lab}$ = 14° to 88°). Over the nearly 170 modules within this angular range, the mean deviation from the energy calibration adopted for this campaign was found to be 4%. The latter calibration had been obtained from a module-by-module fitting of the α-particle spectra produced in the reaction ^{129}Xe + $^{\rm nat}$Sn at 50 MeV per nucleon to the calibrated spectra measured for the identical reaction at GANIL.

Acknowledgments

The authors would like to thank the staff of GSI for providing high-quality carbon beams of the desired low energy. This work was supported in part by the European Community under contract ERBFMGECT950083 and by the BMBF (Bonn) - KBN (Warsaw) Collaborative Agreement in Science and Technology under contract POL-196-96.

References

[1] J. Pouthas, B. Borderie, R. Dayras, E. Plagnol, M.F. Rivet, F. Saint-Laurent, J.C. Steckmeyer, G. Auger, C.O. Bacri, S. Barbey, A. Barbier, A. Benkirane, J. Benlliure, B. Berthier, E. Bougamont, P. Bourgault, P. Box, R. Bzyl, B. Cahan, Y. Cassagnou, D. Charlet, J.L. Charvet, A. Chbihi, T. Clerc, N. Copinet, D. Cussol, M. Engrand, J.M. Gautier, Y. Huguet, O. Jouniaux, J.L. Laville, P. Le Botlan, A. Leconte, R. Legrain, P. Lelong, M. Le Guay,

L. Martina, C. Mazur, P. Mosrin, L. Olivier, J.P. Passerieux, S. Pierre, B. Piquet, E. Plaige, E.C. Pollacco, B. Raine, A. Richard, J. Ropert, C. Spitaels, L. Stab, D. Sznajderman, L. Tassan-Got, J. Tillier, M. Tripon, P. Vallerand, C. Volant, P. Volkov, J.P. Wieleczko, G. Wittwer, Nucl. Instr. and Meth. A 357 (1995) 418.

[2] J.B. Birks, Proc. Phys. Soc. A 64 (1951) 874; J.B. Birks, The Theory and Practice of Scintillation Counting, Pergamon Press, Oxford, 1964.

[3] M. Parlog, B. Borderie, M.F. Rivet, G. Tăbăcaru, A. Chbihi, M. Elouardi, N. Le Neindre, O. Lopez, E. Plagnol, L. Tassan-Got, G. Auger, Ch.O. Bacri, N. Bellaize, F. Bocage, R. Bougault, B. Bouriquet, R. Brou, P. Buchet, J.L. Charvet, J. Colin, D. Cussol, R. Dayras, A. Demeyer, D. Doré, D. Durand, J.D. Frankland, E. Galichet, E. Genouin-Duhamel, E. Gerlic, S. Hudan, D. Guinet, P. Lautesse, F. Lavaud, J.L. Laville, J.F. Lecolley, C. Leduc, R. Legrain, M. Louvel, A.M. Maskay, L. Nalpas, J. Normand, J. Péter, E. Rosato, F. Saint-Laurent, J.C. Steckmeyer, B. Tamain, O. Tirel, E. Vient, C. Volant, J.P. Wieleczko, Nucl. Instr. and Meth. A 482 (2002) 674.

[4] M. Parlog *et al.*, Nucl. Instr. and Meth. A 482 (2002) 693.

[5] D.V. Kamanin *et al.*, FOBOS Collaboration, Nucl. Instr. and Meth. A 413 (1998) 127.

[6] A. Avdeichikov *et al.*, CHICSi Collaboration, Nucl. Instr. and Meth. A 439 (2000) 158.

[7] S. Aiello *et al.*, CHIMERA Collaboration, Nucl. Instr. and Meth. A 369 (1996) 50.

[8] A. Avdeichikov *et al.*, CHICSi Collaboration, Nucl. Instr. and Meth. A 466 (2001) 427.

[9] Y. Larochelle *et al.*, TASCC Collaboration, Nucl. Instr. and Meth. A 348 (1994) 167.

[10] A. Wagner *et al.*, MSU-I Collaboration, Nucl. Instr. and Meth. A 456 (2001) 290.

[11] N. Marie, PhD Thesis (University of Caen), Report GANIL T95 - 04 (1995).

[12] J. Lukasik *et al.*, GSI Report (in preparation).

[13] F. Hubert, R. Bimbot, H. Gauvin, Atomic Data Nucl. Data Tables 46 (1990) 1.

[14] T. Fujisawa, N. Kishida, T. Kubo, T. Wada, Y. Toba, T. Hasegawa, M. Sekiguchi, N. Ueda, M. Yasue, F. Soga, H. Kamitsubo, M. Nakamura, K. Hatanaka, Y. Wakuta, T. Tanaka, A. Nagao, J. Phys. Soc. Japan 50 (1981) 3198.

[15] J.K. Dickens, D.A. Haner, C.N. Waddel, Phys. Rev. 129 (1963) 743.

[16] J.F. Ziegler, Program SRIM-2000 (version 2000.39), accessible at http://www.srim.org.

[17] J. Pouthas, A. Bertaut, B. Borderie, P. Bourgault, B. Cahan, G. Carles, D. Charlet, D. Cussol, R. Dayras, M. Engrand, O. Jouniaux, P. Le Botland, A. Leconte, P. Lelong, L. Martina, P. Mosrin, L. Olivier, J.P. Passerieux, B. Piquet, E. Plagnol, E. Plaige, B. Raine, A. Richard, F. Saint-Laurent, C. Spitaels, J. Tillier, M. Tripon, P. Vallerand, P. Volkov, G. Wittwer, Nucl. Instr. and Meth. A 369 (1996) 222.

Table 1

Comparison of the a_1 coefficients for the modules selected for Fig. 4 with ring number R and module number M. Superscripts refer to the corresponding panels on that figure. The intrinsic errors of the fitting procedure are listed in column 2.

ID	a_1 (channel/MeV)	
R - M	^{12}C+^{1}H	^{129}Xe+^{nat}Sn
06-07^a	$13.19\ ^{+0.14}_{-0.06}$	13.35
07-11^b	$10.43\ ^{+0.11}_{-0.27}$	10.87
08-15^c	$14.74\ ^{+0.25}_{-0.27}$	14.88
09-04^d	$25.06\ ^{+0.35}_{-0.61}$	24.53
10-16^e	$36.32\ ^{+0.03}_{-0.03}$	35.87
10-16^f	$36.31\ ^{+0.08}_{-0.02}$	35.87
11-20^g	$53.98\ ^{+0.85}_{-0.91}$	52.80
12-08^h	$61.63\ ^{+0.40}_{-0.53}$	59.94

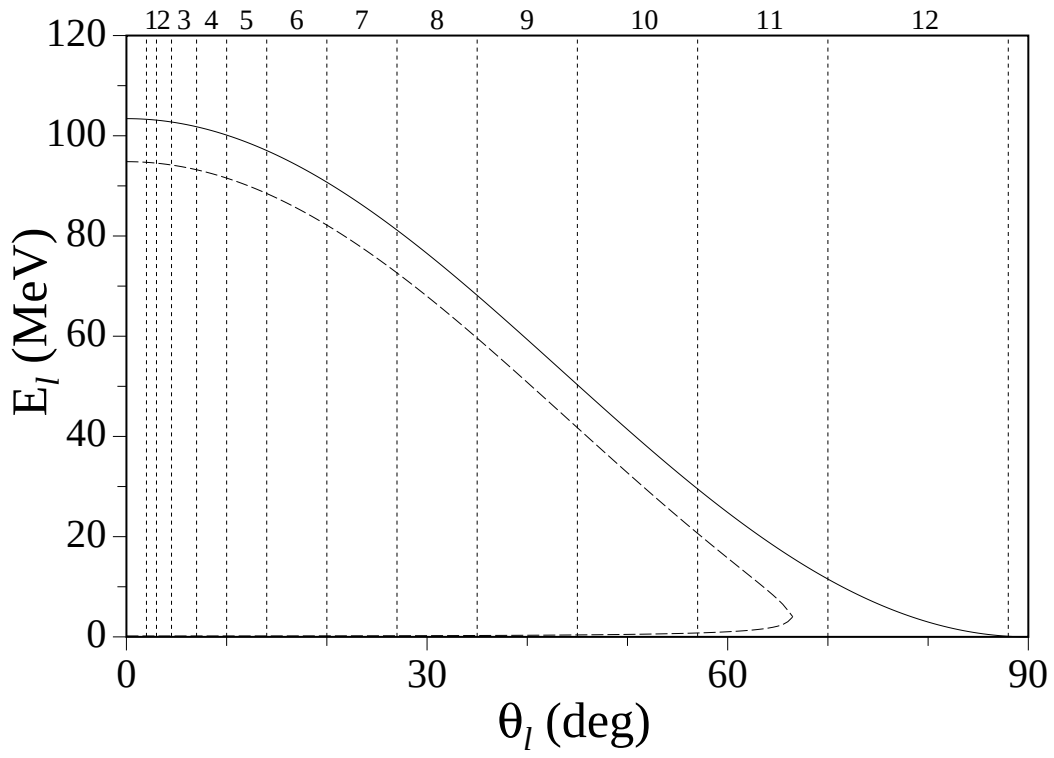

Fig. 1. Energy of the light ejectile as a function of its emission angle for the elastic and inelastic ^{12}C + ^{1}H interactions at $E(^{12}\mathrm{C}) = 30$ MeV per nucleon. The curves are for: elastic (solid line) and inelastic (4.439 MeV state; dashed line) protons. The limits in θ_{l} of the CsI(Tl) detector acceptances, for the INDRA rings with the indicated numbers, are marked with the vertical dotted lines.

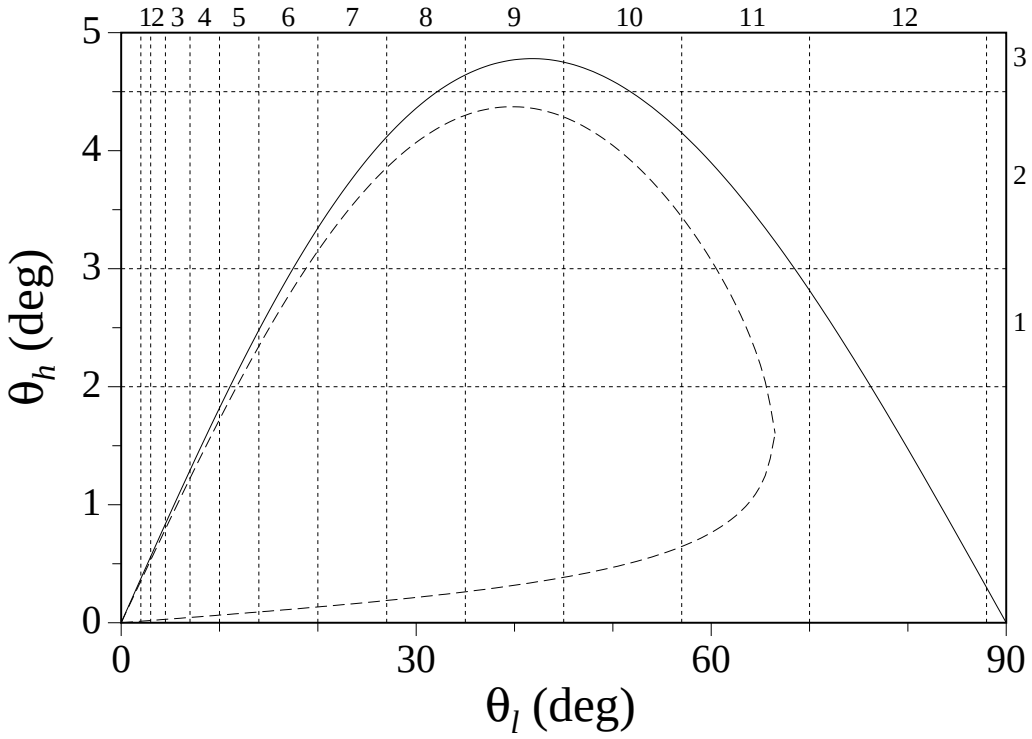

Fig. 2. Correlation of the emission angles of the heavy and the light ejectile in binary reactions following ^{12}C + ^{1}H interactions at $E(^{12}\mathrm{C}) = 30$ MeV per nucleon. The curves are for: elastic (solid line) and inelastic (4.439 MeV state; dashed line) protons. Vertical and horizontal dotted lines mark the limits of the module acceptances in polar angle, θ, for the INDRA rings with the indicated numbers.

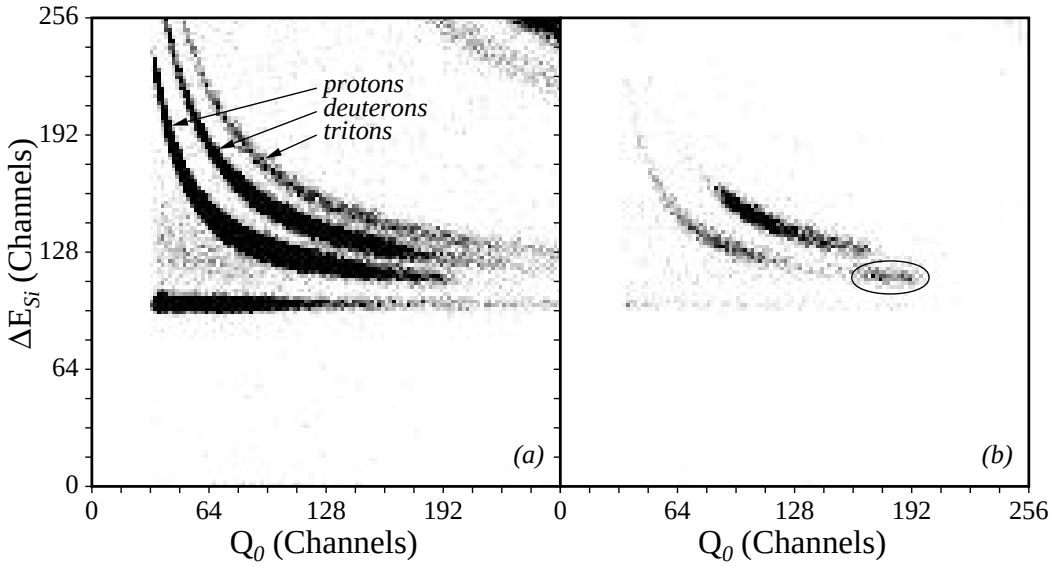

Fig. 3. (a) Inclusive two-dimensional spectrum $\Delta E_{\rm Si} - Q_0$, silicon-high gain vs CsI(Tl)-total collected charge, for particles detected in ring 7 module 4, displaying hyperbolae due to the hydrogen isotopes. (b) Light ejectiles selected in (a) by requiring a coincidence with a particle detected in ring 2 module 15. The proton groups referred to in the text are encircled.

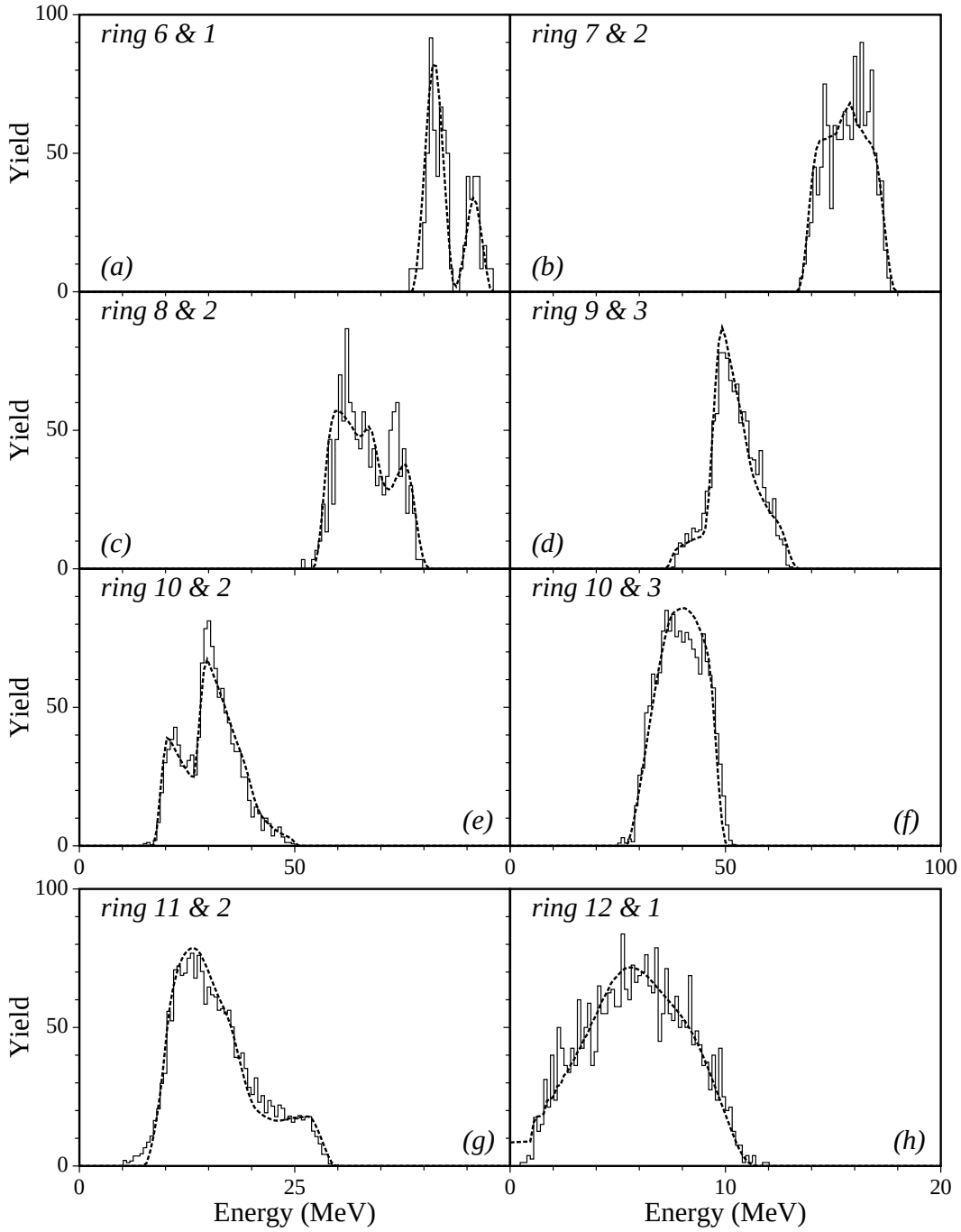

Fig. 4. (a) - (h) Coincident spectra for protons from individual modules (histograms), calibrated in energy by fitting to the results of Monte-Carlo simulations (dashed lines). The numbers in the upper left corner of each panel indicate the ring numbers of the coincident proton and ^{12}C detection, respectively.

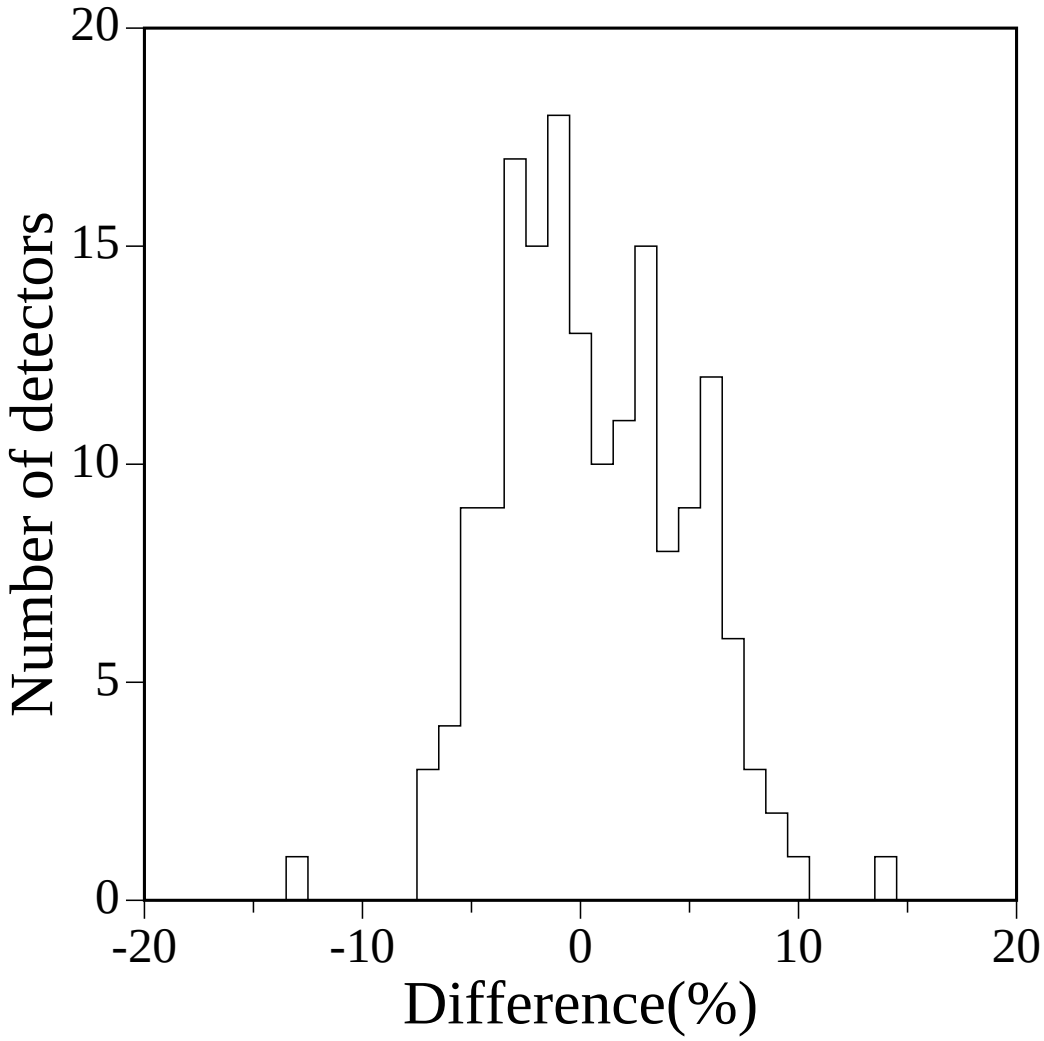

Fig. 5. Distribution of differences of centroid energies resulting from differences in a_1 coefficients, as determined with the two calibration procedures described in the text, for all CsI(Tl) modules in rings 6 to 12.